

peaks. Apparently what Krishnan and Ramanathan meant was the centre of the side of the band with peak at 1285 cm^{-1} . But this is an equally untenable position. All the arguments in my earlier letter still hold if one replaces "minimum of absorption" by "centre of the long-wave side of the absorption maximum". Even their much milder statement in the above letter that "the absorption associated with the 1332 cm^{-1} frequency is an integral part of the $8\text{ }\mu$ band" is open to question, as it depends on (a) the resolving power of the spectrometer used, and (b) the temperature at which the measurements are made.

It is quite possible that at very low temperatures these bands may sharpen so much that the 1332 cm^{-1} frequency cannot even be said to lie on the side of a band.

G. B. B. M. SUTHERLAND.

Laboratory of Colloid Science,
Cambridge.
March 29.

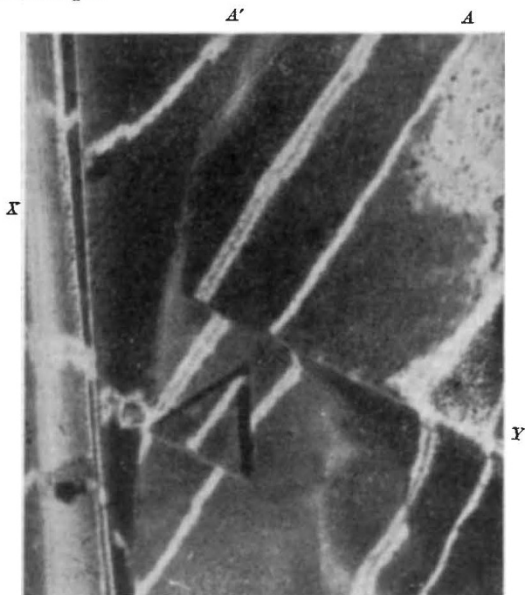
Topography of the Face of a Diamond Crystal

WE have applied the multiple-beam interference technique described earlier¹ to the study of the topography of a natural octahedron face of a diamond, thus revealing considerable information about growth, etch, face curvature, etc. We have settled a fifty-year-old controversy concerning the origin of the beautifully regular shallow-pit triangular markings shown by such faces. Miers² cautiously stated that these are supposed to be due to etching and shows them pointing to the octahedron edge. Fersmann and Goldsmidt³ asserted that etch or solution can be responsible both for the triangles and the curved faces. Williams⁴ proposed on rather slender grounds that the triangular pits and curved faces arise from growth and not from solution.

We have now proved that a typical characteristic triangular pit is due to growth.

During the progress of the work, a novel interference method has been developed which will be described as a 'crossed fringe' technique. This simplifies and speeds up the analysis.

The optical flat is first set as near parallel as possible to the diamond face, giving maximum fringe dispersion and maximum sensitivity. All the visible mercury radiations are used, the result being the production of multiple-beam interference fringes which reveal in a striking manner much sub-microscopic topographical detail. It is not possible from such a picture to obtain much numerical information about the heights (depths) of features. However, an area of uniform tint means that such an area is of uniform height (depth) to within a very small fraction of a light wave. A change of only $\lambda/200$ can produce a tint alteration. The flat is then slightly tilted relative to the crystal, leading to the formation of sharp, widely spaced multiple-beam fringes¹. These are photographed superposed on the high dispersion fringes.



The accompanying reproduction illustrates the technique, which permits of a rapid exact evaluation of the structure. The area represented is about 1 sq. mm. Attention is directed to the extreme fringe sharpness, AA' being successive orders for the green line of mercury, with the yellow doublet between.

Among other features, the reproduction shows a clearly marked triangle in the lower half. (Fringe displacement to the right here means an elevation.) The fringe from A continues unbroken until reaching the ridge XY at which it is displaced to the right. But the fringe through the triangle is quite clearly a linear continuation of A , hence the triangle base is at the same level as the large uniform area above XY . The depth of this particular triangle is only $440\text{ }\text{\AA}$. Other triangles, of different depths, show the same effect. It is completely unreasonable to postulate a hypothetical etching that takes place down to the somewhat removed outside level. Nor can one suppose

that simultaneous etch continues down to hypothetical abnormally resisting layers (at different levels for different features). This would be a highly improbable state of affairs indeed.

It is certain therefore that the area below XY has grown in the form of three plane waves inclined at 60° to each other. The arresting of such growth can lead to the formation of equilateral triangles (which may be and are occasionally truncated to hexagons). The triangle shown thus arises entirely through failure of the completion of the growth sheets, below XY , and etching has nothing to do with it. This particular triangle points to the octahedron edge.

A number of these triangular growth-pits have been measured, and depths ranging from some 60 to 600 \AA . found, that is, some 30-300 atom layers.

We have also found in addition distinct evidence of the existence of etching or solution, leading to the formation of irregular shallow hollows of arbitrary orientation. This will be discussed elsewhere.

Successive stepped growth-sheets are also clearly visible, and it is of considerable interest that these frequently grow in a stepped pyramid leading effectively to a curvature of the vicinal face, at times considerable. We believe that the well-known curvature of diamond faces and edges is also probably a growth effect.

We note that a previous attempt has been made to examine diamond topography by interference, but this⁵ was effectively only a two-beam interference method and as such was completely inadequate for the purpose, showing only the coarsest of features and revealing little not already shown by the microscope.

A full report of the analysis of the mass of detail revealed by the precision multiple-beam 'crossed fringes' will be communicated elsewhere. Particular attention is directed to the very considerable saving in labour due to this technique.

We thank Mr. P. Grodzinski of the Diamond Trading Company for the loan of the diamond and for mounting it for us.

S. TOLANSKY.
W. L. WILCOCK.

Physics Department,
University,
Manchester.
March 7.

¹ Tolansky, *Nature*, **159**, 722 (1943); *Proc. Roy. Soc., A*, **184**, 41 (1945).

² Miers, "Mineralogy" (1902).

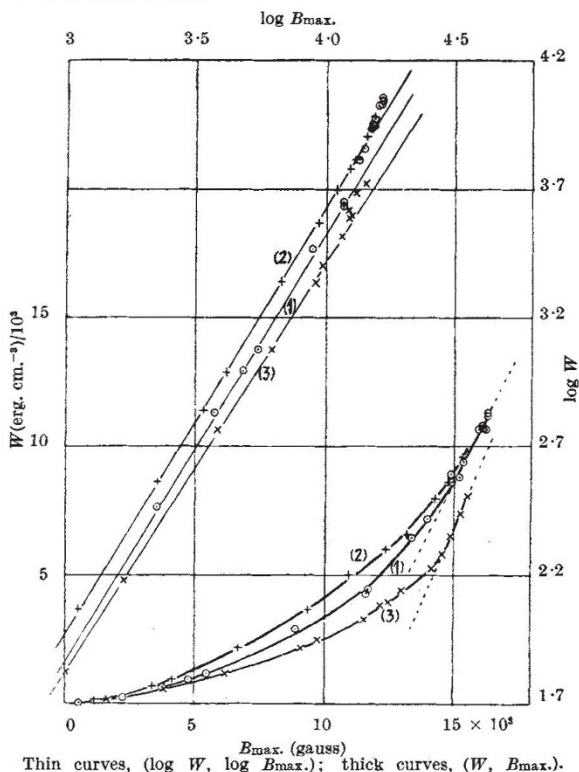
³ Fersmann and Goldsmidt, "The Diamond" (1911).

⁴ Williams, "Genesis of the Diamond" (1932).

⁵ Kayser, *Indust. Diamond Rev.*, **4** (Jan. 1944).

Loss Due to Magnetic Hysteresis in Silicon-Steel Sheets

WE have determined magnetic hysteresis loops by the ring-ballistic method for three different sheets of silicon-steel in an extensive range of values of magnetic flux-density B_{max} . (B_{max} is the flux-density corresponding to the cusp of the loop). From these loops we have derived the energy loss W , in ergs per cubic centimetre per cycle for different values of B_{max} , and by plotting those values against the corresponding values of B_{max} , we obtained the accompanying curves for three sheets of steel.



If Steinmetz's empirical law ($W = \eta(B_{\max})^k$ ($k \approx 1.6$) is applicable to our experimental data, then there must exist a linear relation between $\log W$ and $\log B_{\max}$; we find such a linear variation, with the approximate error of 1 per cent, between the flux-densities of 1,000 and 12,000 gauss, with the following values for the constants η and k :

	Sheet 1	Sheet 2	Sheet 3
η	0.00076	0.0010	0.0011
k	1.66	1.65	1.59

It was found that Steinmetz's law is not applicable at high and low flux-densities. We have observed, like Brailsford¹, that for sheets 1 and 3, and very high values of B_{\max} , the hysteresis loss increases with B_{\max} according to a linear law.

Moreover, it has been shown experimentally that, in accordance with theory, the influence of a superimposed steady unidirectional flux on the hysteresis loss is nil. The measurements were carried out with steel sheet 1 and for three different values of steady flux: 1,500, 4,100 and 11,300 gauss. 4,100 gauss is the value of the flux-density for which magnetic permeability of the material is a maximum. As an example, the experimental data for two loops of very different shape are: loop with steady flux = nil: $B_{\max} = 13,360$ gauss; $W = 6.47 \times 10^8$ erg.cm.⁻²; loop with steady flux = 11,300 gauss: $B_{\max} = 13,320$ gauss; $W = 6.31 \times 10^8$ erg.cm.⁻².

S. VELAYOS.
V. SANCHEZ-GIRON.

Physical Laboratory,
University of Valladolid,
Jan. 8.

¹ Brailsford, F., *J. Inst. Elect. Eng.*, **90**, 313 (1943).

Biological Action of Radiations

It has been shown previously¹ that when radiation (for example, X-rays, α -particles, neutrons) is absorbed in aqueous solutions, an indirect chemical effect is produced due to the formation of free radicals and atoms:



In general, this is followed by the recombination:



and by interactions of these radicals with other acceptor substances (S , S_1 , S_2 , ...) present, for example:



This scheme of reactions must exist also in the aqueous systems of biological subjects. From the point of view of the older 'hit' theory², reaction (3) corresponds to a single 'hit', while if, for example,

$$E_1 = S_1, E_2 = S_2, \dots, E_{n-1} = S_{n-1} \quad (4)$$

one gets a successive change of the (starting) substrate (S) by 1, 2, ..., n interactions with, for example, OH radicals, which are equivalent to 1, 2, ..., n 'hits'. It can be shown that—under certain conditions—there is a complete formal analogy between the 'hit' theory, which is described by Poisson's formula, and the mathematical expression for the above system of equations (3, 3.1, ..., 3.n).

If the biologically active substance is represented by the molecule S , the essential interaction corresponds to equation 3 and the theory suggests two important cases:

Case A. The recombination process (2) can be neglected (if the interaction with the acceptor molecules is relatively fast). From the above scheme of reactions, it follows that in this case the action of the radiation (for example, the half 'lethal' dose $D_{1/2}$) depends only on the total number of ions (radicals) produced, independent of the nature and wave-length of the radiation. This case is represented, for example, by the mutations induced by X-rays. Under the assumption—which is almost certainly fulfilled—that apart from the S molecules there are also some other (biologically non-active) molecules present which react with the OH-radicals (thereby exerting a 'protection effect') the chemical theory leads to the equation:

$$S = S_0 \exp. (-\alpha D) \quad (5)$$

where S and S_0 represent the numbers of these molecules at times t and zero respectively; D , the total dose of radiation and:

$$\alpha = \ln 2/D_{1/2} \sim q_s(q_{sm}[S_m])^{-1} \quad (6)$$

where q_s represents the (kinetic) cross-section of the S molecules and the term in brackets can be interpreted as the mean linear region available per one molecule of the (protecting) substrate molecules (S_m).

Case B. Recombination reaction (2) taken into account (if the radicals are present in relatively high concentrations or, for example, the acceptor molecules are relatively non-reactive). It follows that in this case the local concentration and distribution of the radicals is of importance. While for different radiations the number of ions (radicals) produced is approximately the same for equal doses, their local distribution may differ widely. In this case, therefore, the action of the

radiation must depend on the nature of the radiation, as is known to be the case, for example, of the lethal effect on unicellular organisms.

The above scheme leads to the following expression (with certain simplifying assumptions):

$$S = S_0 \exp. \left(- \frac{k_3 D}{k_2 [H]_l} \right) = S_0 \exp. (-\alpha D) \quad (7)$$

where $[H]_l$ represents the local concentration of the radicals in the regions where the actual reaction takes place. As a first approximation $[H]_l$ can be estimated for two important stages of the reaction. (i) *In the initial stage*, that is, before any appreciable diffusion of the radicals (formed in the tracks of the ionizing particles) has set in. Here one may assume that:

$$[H]_{l(i)} \propto \text{number of ions per unit length of track} \quad (8)$$

This quantity is known experimentally^{3,4} for different radiations. More generally, one has approximately^{5,6} (if V denotes the energy of the radiation):

$$[H]_{l(i)} \propto V^{-1} \text{ (for X-rays)} \quad (9)$$

$$[H]_{l(i)} \propto V^{-1/2} \text{ (for } \alpha\text{-rays)} \quad (9a)$$

(ii) *In the advanced stage* (but before any appreciable intermixing of the individual ionization tracks has occurred):

$$[H]_{l(ii)} \propto V \quad (10)$$

Taking into account both these stages for the action of, say, X-rays, one obtains for α of equation 7,

$$\alpha = \alpha_{(i)} + \alpha_{(ii)} \propto \frac{k_3}{k_2} \frac{1}{V} \left(\frac{V^2}{a} + 1 \right) \quad (11)$$

where a denotes a proportionality factor. Remembering that $V \propto \lambda^{-1}$ and that for the range (R_e) of the (ionizing) fast electrons one has the relation⁷: $R_e \propto V^2$, one obtains finally from equations 7 and 11

$$D_{1/2} = \ln 2/\alpha \propto \frac{1}{\lambda} \frac{a}{(R_e + a)}, \quad (12)$$

which is formally identical with Glocker's well-known expression.

It is now possible to predict that if sufficiently hard γ -rays or X-rays are used, the dependence on the wave-length should gradually diminish and finally disappear. This can be illustrated by Wyckoff's own figures⁸ for *Bacterium coli*, where the mean lethal dose decreases in the series of decreasing wave-length as: 8.4, 6.67, 4.65, $4.20 \times 10^4 r$, and in order to achieve the same effect with α -rays, $24 \times 10^4 r$ are required. On the other hand, while it is known that the doses of radiation for the production of mutations are independent of the wave-length in the case of γ - and X-rays⁹ a much higher dose of neutrons is required to produce the same effect¹⁰. This follows directly from the above theory, as the recoil protons produce a relatively high local ion (radical) density leading to increased recombination.

A full account will be published elsewhere which will include also a discussion of 'multiple hit effects', where the situation is somewhat different¹¹.

JOSEPH WEISS.

King's College,
University of Durham,
Newcastle-upon-Tyne.
Jan. 25.

¹ Weiss, *Nature*, **153**, 748 (1944).

² cf. Mayneord, *Proc. Roy. Soc. A*, **146**, 867 (1934).

³ cf. Gray and Read, *Brit. J. Radiol.*, **15**, 72 (1942).

⁴ Lea, *Proc. Camb. Phil. Soc.*, **30**, 80 (1934); *Brit. J. Radiol.*, **16**, 338 (1943).

⁵ cf. Bethe and Bacher, *Rev. Mod. Phys.*, **8** (1936).

⁶ Bagge, *Ann. Phys.*, **30**, 72 (1937).

⁷ Glocker, *Z. Phys.*, **77**, 653 (1932).

⁸ Wyckoff, *J. Exp. Med.*, **51**, 921 (1930); **52**, 435, 769 (1930).

⁹ cf. Schrödinger, "What is Life?" (Cambridge, 1944).

¹⁰ Timoféeff-Ressovsky and Zimmer, *Naturwiss.*, **26**, 362 (1938).

¹¹ cf. Hevesy, *Rev. Mod. Phys.*, **17**, 102 (1945).

Effect of Container Walls on Packing Density of Particles

IN recent correspondence¹ in *Nature* a general theorem on the ordered packing of equal spheres is cited as implying that "the overall voidage of any one of the four possible ordered arrangements of equal spheres packed into a container is independent of the relative size of the container provided its size and shape are such that it will contain an integral number of 'unit' cells of the particular ordered arrangement and in all other cases an ordered packing cannot be obtained". This is due to a misconception of the 'unit' cell, which in the first three out of the four ordered packings, namely, a sphere having 12, 10, 8 or 6 neighbours, really contains fractions of a sphere totalling to one, and it is only in the fourth case that the unit cell, being a simple cube, contains a whole sphere.

Furthermore, the inescapable higher voidage adjacent to the container walls as compared to the interior of the container has to be taken into account², and its contribution to the overall voidage has to be allowed for; unless it happens to be negligible, as with a container of very large size compared to the particle size of the packed material. Characteristic voidage for a compacted packing of a sized material is then found to depend more on the particle shape^{3,4,5} than on the particle size. This increases with increased deviation of the irregular particles from a spherical shape, unless conditions exist to